New developments in the spatial encoding of spin interactions for single-scan 2D NMR‡

Yoav Shrot,† Assaf Tal† and Lucio Frydman*

Single-scan 2D NMR relies on a spatial axis for encoding the indirect-domain internal spin interactions. Various strategies have been demonstrated for fulfilling the needs underlying this procedure. All such schemes use gradient-echoed sequences that leave at their conclusion solely the effects of the internal interactions along the indirect domain; they also include a real-time scheme that though simple, yields in general mixed-phase line shapes. The present paper introduces two new proposals geared up for easing the spatial encoding underlying single-scan 2D NMR methodologies. One of these is capable of delivering dispersive-free peaks along the indirect domain, and thereby purely-absorptive 2D line shapes, in amplitude-encoded experiments. The other demonstrates for the first time, the possibility to obtain single-scan 2D spectra without echoing the effects of the encoding gradient – simply by applying a single-pulse frequency sweep to encode the interactions. Both of these modes are compatible with homo- and heteronuclear correlations, and exhibit a number of complementary features *vis-à-vis* encoding alternatives that have so far been presented. The overall principles underlying these new spatially encoding protocols are derived, and their performance demonstrated with single-scan 2D NMR TOCSY and HSQC experiments on model compounds. Copyright © 2009 John Wiley & Sons, Ltd.

Keywords: NMR; ultrafast 2D NMR; spatial encoding; purely-absorptive lineshapes; frequency-swept RF pulses

Introduction

Two-dimensional (2D) spectroscopy stands at the core of NMR's analytical applications in chemistry and biochemistry.[1–3] The classical 2D NMR experiment relies on a time-domain acquisition whereby an initial evolution parameter t_1 encodes the indirect-domain Ω_1 interactions, whereas a physical time t_2 monitors the direct-domain frequencies Ω_2.[4,5] Given the parametric examination of the indirect domain evolution, the collection of numerous t_1-incremented scans becomes an integral part of this data-acquisition mode. Recent years have witnessed a number of alternatives to this acquisition scheme, aimed at reducing the minimal number of scans needed to obtain the desired spectral information.[6–8] Included among these methods counts an 'ultrafast' approach, capable of delivering arbitrary 2D NMR spectra within a single scan.[9–11] Ultrafast 2D NMR operates by replacing the serial t_1-incrementation with a single-scan encoding of the interactions along a spatial z-axis. The equivalent of a full shift or coupling indirect-domain evolution can then be imparted, by the combined application of a suitable G_e magnetic field gradient spreading frequencies as $\gamma_e G_e z$, and of frequency-selective radiofrequency (RF) pulses exciting spins over time as a function of their positions z. In other words, instead of having a particular shift or coupling Ω_1 imparting a uniform phase $\phi(t_1) = \Omega_1 \cdot t_1$ to spins throughout the sample, single-scan 2D NMR imparts an analogous encoding but along a spatial axis:

$$\phi(z) = C\Omega_1 \cdot (z - z_0) \qquad (1)$$

where C and z_0 are two parameters under the experimentalist's control. Figure 1(A) exemplifies a common scheme that on the basis of these principles can be used to impart an amplitude-modulated spatial encoding of this sort. As explained in further detail elsewhere[12,13] the equal RF sweeps in this sequence act on

the sample of length L over excitation and storage periods $t_1^{max}/2$, to impart an amplitude modulation of a site's magnetization of the form

$$M(z) = M(\Omega_1) \cdot \cos[C\Omega_1(z - L/2)] \exp[-C(z - L/2)/T_2] \qquad (2)$$

with $C = t_1^{max}/L$. When inserted within the framework of a 2D NMR acquisition, the spatial Ω_1-modulation stemming from this encoding will be coherently transferred through the sequence's mixing period, and in general result in a null detectable signal after considering its integration over a $-L/2 \le z \le +L/2$ range. Ultrafast NMR, however, implements its detection while subjecting the sample to an acquisition field gradient G_a, possessing the same spatial geometry as the initial encoding gradient G_e. The observable NMR signal S then becomes a simultaneous function of the direct-domain time t_2 as well as of a $k = \gamma_a \int_0^t G_a(t')dt'$ acquisition wavenumber. This gradient-driven decoding performs the analog of a Fourier transformation (FT) on the spatially encoded

---

* Correspondence to: Lucio Frydman, Department of Chemical Physics, Weizmann Institute of Science, 76100 Rehovot, Israel.
  E-mail: lucio.frydman@weizmann.ac.il

† Contributed equally to this work.

‡ This article was published online on 24 February 2009. An error was subsequently identified. This notice is induced in the online and print versions to indicate that both have been corrected, 4 March 2009.

Department of Chemical Physics, Weizmann Institute of Science, 76100 Rehovot, Israel

(A) "First-in, last-out" encoding   (B) "First-in, first-out" encoding
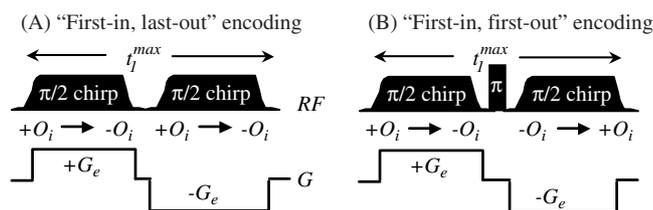
Figure 1. Comparison between (A) the original amplitude-modulated scheme yielding a 'first-in, last-out' linear spatial encoding (12) and (B) the new 'first-in, first-out' scheme discussed in this work, whereby spins at all positions spend equal times precessing in the transverse plane (and thereby are affected to the same extent by the T_2 decay) yet a linear $C\Omega_1 z$ encoding is still achieved with a $C = \frac{t_1^{max}}{L}$ efficiency. [Correction made here after initial online publication]

indirect-domain evolution, leading to a signal

$$S[k(t)] \propto M(\Omega_1) \int_{-L/2}^{+L/2} \{\cos[C\Omega_1(z - L/2)] \exp[-C(z - L/2)/T_2]\}$$

$$\exp[ik(t)z]dz$$

$$\approx M(\Omega_1)\delta[k \pm C\Omega_1] \qquad (3)$$

As δ here will be a relatively sharp point-spread function, Eqn (3) will provide well-defined Ω_1-specific echoes whenever $k = |C\Omega_1|$. Such echoes will reveal the nature of the indirect-domain evolution frequencies, transforming the k wavenumber into the equivalent of a ν_1 indirect-domain frequency axis. Two-dimensional NMR spectra can then be retrieved within a single scan by oscillating the k-value – i.e. by oscillating the G_a decoding gradient. Monitoring the modulations imparted by the Ω_2 direct-domain evolution frequencies on the resulting train of k-domain echoes as a function of $t = t_2$, thereby provides an interferogram which by FT *versus* t_2 results in the $I(\nu_1, \nu_2)$ spectrum being sought.

In spite of its simplicity and robustness, the scheme in Fig. 1(A) possesses a number of features that justify the search for alternative encoding schemes. One of them relates to the $\exp[-C(z - L/2)/T_2]$ relaxation decay term affecting the spin evolution, which by weighting the signal asymmetrically with respect to $z = 0$ will lead to dispersive components along the k-domain for the echoes represented by Eqn (3). When considering the FT *versus* t_2 that leads to the final $I(k/\nu_1, \nu_2)$ 2D spectrum, these dispersive components may in turn translate into mixed-phase line shapes.[14] Another problem relates to the $z_0 = L/2$ spatial offset modulating the coherent $C\Omega_1(z - L/2)$ evolution, which (akin to a shift in the origin of the time axis in conventional FT NMR experiments) will be associated to a strong linear phase-distortion of the k-echoes, and thereby of the 2D peaks. A final feature worth highlighting – not just of this model sequence but in fact of all sequences hitherto proposed to implement single-scan 2D NMR[10,15–19] – relates to the need to echo the encoding gradient via a $\pm G_e$ oscillation, in order to leave solely an internal Ω_1 encoding of the kind demanded by Eqn (1). The present paper explores further all these issues by introducing two new approaches to implement the indirect-domain spatial encoding required by single-scan 2D NMR. The first one involves a modification of the sequence in Fig. 1(A), capable of delivering an amplitude-modulated encoding of the interactions which, however, now appears evenly weighted

about $z = 0$. By virtue of this the δ function in Eqn (3) becomes purely real, leading to purely-absorptive lines when considering the 2D trace. The second approach shows, for the first time, the feasibility of obtaining single-scan 2D NMR spectra even if the encoding departs from the linear $\Omega_1 z$-dependence of Eqn (1) which has guided the development of ultrafast 2D NMR thus far. The principles underlying these new approaches are described in the following paragraphs, and their performance illustrated with a variety of single-scan 2D NMR acquisitions.

Experimental

The schemes presented in this work were tested on a Varian iNova® 500-MHz NMR spectrometer equipped with an inverse triple-resonance probehead. The chirped RF and pulsed gradient manipulations needed for their execution were implemented via phase- and amplitude-modulating tables, generated *a priori* using custom-written Matlab® software subroutines and then transferred to the spectrometer for execution. Similar files, however, can also be generated using Varian- or Bruker-supplied pulse-shaping utilities such as '*Pbox*' or '*Stdisp*'.[20] All data processing as well as ancillary spin simulations were carried out using custom-written Matlab® packages, which can be made available upon request.

Results

Amplitude-modulated encoding with purely-absorptive line shapes

To better appreciate the operating principles of the new sequences to be introduced here, it is convenient to summarize first the physical principles of schemes which, as the one in Fig. 1(A), have already been analyzed.[13] This sequence achieves its spatial encoding by beginning the spins' excitation at one end of the sample, and proceeding monotonically with a progressive $\pi/2$ nutation all the way to the opposite extreme by chirping the RF pulse while in the presence of a gradient $G_e \hat{z}$. This RF pulse consequently requires its amplitude calibrated to a $\pi/2$ rotation[21,22] and its offset swept in a constant, time-dependent fashion $O(t) = O_i + R \cdot t$, where O_i is an initial frequency value and R the offset sweeping rate. This RF will affect spins as a function of position, whenever its offset matches the z- and Ω_1-specific resonance condition

$$\Omega_1 + \gamma_e G_e z = O(t) \qquad (4)$$

At this particular instant, which we refer to as $t_+(z)$, spins positioned at z will be excited and begin to precess. This will happen under the effects of the shifts/couplings Ω_1 that one is trying to measure, as well as under the action of the ancillary gradient G_e which remains active throughout the remainder of the chirp. Moreover, also the T_2 effects defining the δ peak-shape will begin to act at this excitation point. As described in Ref. [12], an evolution that is linearly dependent on $\Omega_1 z$ but that is free from gradient effects as required by Eqn (2) can be achieved by introducing a second RF sweep – identical to the one used to impart the initial $\pi/2$ excitation, but acting in the presence of an opposite gradient – $G_e \hat{z}$. This second element will create an RF-driven storage of the spins' coherences and, owing to the $+G_e \rightarrow -G_e$

reversal, it will proceed in a 'first-in, last-out' fashion. Indeed, owing to the gradient's reversal, the instant $t_-(z)$ at which this second storage pulse operates will mirror closely what occurred in the initial excitation period. Therefore during its course, spins will evolve under the action of an Ω_1 interaction that will accumulate and of a gradient interaction that progressively echoes away, until the instant when this latter contribution reaches zero. At this point, the component of the spin coherence that is perpendicular to the RF field becomes longitudinally stored, and all spin evolution ceases. Both the overall $t_1(z) = [(t_1^{max}/2) - t_+(z)] + t_-(z)$ evolution time as well as the associated T_2 relaxation effects will hence be largest for one end of the sample and smallest for the opposite one, leading to the $z_0 = L/2$ effects in Eqn (2) and to the mixed-phase distortions noted earlier.

A solution to the asymmetry introduced by this 'first-in, last-out' encoding scheme would arise if switching to a 'first-in, first-out' scheme; i.e. to a strategy where the first z-position to be excited would also be the first one to be stored, and where the last voxel to be excited would also be the last one to be frozen. When generalized over all $-L/2 \leq z \leq +L/2$ positions, this would imply that all spins will have spent equal amounts of time precessing in their transverse planes; the effects of T_2 relaxation on any given site would thereby become constant throughout the sample, and the dispersive components arising upon FT-ing such constant envelop would disappear from the ensuing k-domain echoes. From a practical perspective, a naïve analysis would suggest implementing this 'first-in, first-out' strategy by either reversing the senses of the RF sweep directions for the $\pm G_e$ chirped pulses, or by applying two identical RF under equal gradient values. More careful examinations, however, reveal that in either of these cases a quadratic gradient-derived term, rather than the internal $\Omega_1 \cdot z$ linear function, would become the dominant feature of the evolution phase. Still it is possible to achieve such scheme – preserving the desired $\Omega_1 z$ information while eliminating undesired G_e-derived quadratic phase terms – by introducing onto the reversed-gradient/reversed-RF-sweep scheme just mentioned, an additional hard π pulse refocusing in between the two reversed chirps (Fig. 1(B)). Using terminology and arguments introduced elsewhere,[13] one can then describe the phase accrued by spins at specific positions z during the course of the initial $\pi/2$ excitation sweep as

$$\phi_{exc}(t,z) = \begin{cases} 0 & 0 \leq t \leq t_+(z) \\ \phi_{rf}[t_+(z)] + (\Omega_1 + \gamma_e G_e z) & t_+(z) \leq t \\ \cdot [t - t_+(z)] & \end{cases} \quad (5)$$

where $t_+(z) = \dfrac{\Omega_1 + \gamma_e G_e z - O_i}{R}$ is the time elapsed from the beginning of the chirped pulse application, and $\phi_{rf}(t) = \int_0^t O(t')dt' = O_i \cdot t + \frac{1}{2} R \cdot t^2$ the total phase accumulated by frequency-swept RF until the nutation of the spins. Assuming that R has been tuned so as to sweep a range going from $O_i = -\gamma_e G_e L/2$ to $O_f = +\gamma_e G_e L/2$ over a time $t^{(\pi/2)} \approx t_1^{max}/2$, then the total phase accumulated by spins at the conclusion of the $t^{(\pi/2)}$ excitation period can be written as

$$\phi_{exc}(t^{(\pi/2)}, z) = (\Omega_1 + \gamma_e G_e z) \cdot t^{(\pi/2)} - \frac{(\Omega_1 + \gamma_e G_e z - O_i)^2}{2R} \quad (6)$$

Notice here the foretold quadratic z^2 dependence, which at this point we are trying to eliminate. The sequence continues with the application of a hard π pulse effectively reversing all dynamic phases, and of a spin evolution taking place under the effects

of the same internal couplings but in the presence of a reversed external gradient. Taking these facts into consideration one can describe the dynamic evolution phases accrued by spins during the course of the second, storage RF pulse, as

$$\phi_{storage}(t,z) = -\phi_{exc}(t^{(\pi/2)}, z) + (\Omega_1 - \gamma_e G_e z) \cdot t \quad (7)$$

Since this second RF pulse executes a storage process, only the component lying perpendicular to the RF will be preserved as a longitudinal state. Denoting $t_-(z) = \dfrac{\Omega_1 - \gamma_e G_e z + O_i}{-R}$ as the instant at which the second RF sweep reaches this storage condition for spins at a position z – notice the reversal in both the gradient and sweep rate signs between the definitions of $t_+(z)$ and $t_-(z)$ – one thus ends up with a longitudinal magnetization component

$$M_{stored}(z) \sim \cos\{\phi_{store}[t_-(z), z] - \phi_{rf}[t_-(z)]\} \quad (8)$$

This coherent evolution component will be weighted by a relaxation decay that will depend on the time t_1 during which T_2 was active. For this 'first-in, first-out' approach this time equals $\dfrac{t_1^{max}}{2}\left(1 + \dfrac{2\Omega_1}{\gamma_e G_e L}\right)$ for every position in the sample; when factoring this together with all the explicit z dependencies appearing in Eqn (8) and considering that usually $\Omega_1 \ll \gamma_e G_e L$, the overall magnetization pattern ends up being

$$M_{stored}(z) = M(\Omega_1) \cos\left[\frac{t_1^{max}}{L}\left(\Omega_1 + \frac{\gamma_e G_e L}{2}\right) z\right] \exp[-\frac{t_1^{max}}{2T_2}] \quad (9)$$

This magnetization exhibits a number of similarities and differences, vis-à-vis the conventional amplitude-modulated spatial encoding pattern arising from Fig. 1(A) and leading to Eqn (2). The most important similarity is that the spatio-temporal factor in Eqn (9) is once again $C = \dfrac{t_1^{max}}{L}$, highlighting the equal encoding efficiencies per unit time of both approaches. On the other hand the relaxation decay term has now become spatially independent; an acquisition gradient acting on such function will therefore result in Fourier-conjugate k/ν_1-domain line shapes that are free from dispersive components for each site. Purely-absorptive peaks should thus be amenable in the ensuing single-scan 2D spectrum. A second noteworthy difference is the absence of the $z_0 = L/2$ factor in the amplitude modulation, which upon considering the k-driven FT should in turn free the indirect-domain line shapes from the large first-order phase distortions that previously affected them. This should also translate in more easily obtainable purely-absorptive 2D peaks. A final main feature worth highlighting is the presence of a new $\dfrac{\gamma_e G_e L}{2}$ shift-like term arising in Eqn (9), adding to the Ω_1 modulation being sought. This extra winding is known a priori, and can easily be compensated by the introduction of short purging pulses along the free evolution periods of the 2D NMR sequence.

To appreciate the potential benefits arising upon utilizing this new encoding scheme, Fig. 2 compares a pair of 2D ^{1}H NMR spectra collected using two forms of spatial encoding. Shown in Fig. 2(A) are mixing-less and TOCSY 2D single-scan NMR spectra obtained using the traditional encoding introduced in Fig. 1(A), where the weight of T_2 relaxation is maximum at one end of the sample and minimum at the other. The relatively wide peak shapes arising
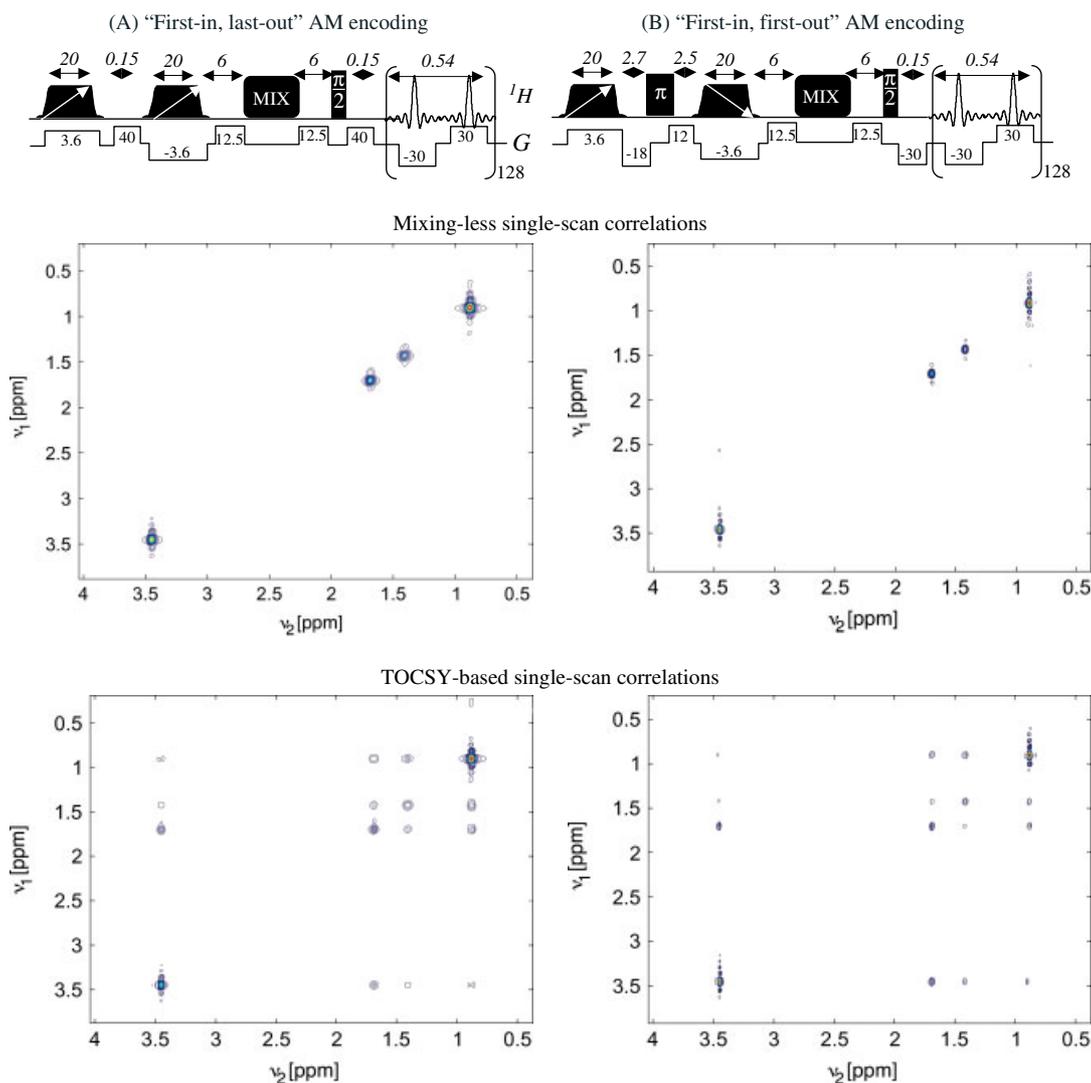
Figure 2. Outcomes observed upon applying the single-scan 2D NMR principles introduced in Fig. 1, to an *n*-butylchloride/CDCl₃ sample. Shown on top are the traditional (left) and newly proposed (right) encoding sequences used in these tests, with gradients and timing parameters (in G/cm and ms) indicated. White arrows represent the relative directions of the 30-kHz-wide sweeps used for excitation and storage. Notice the addition of gradient purging pulses to the schemes of Fig. 1. The central- and lower-panel spectra differ by the absence and presence of a 60-ms-long DIPSI-based mixing sequence[23] respectively. In all cases the 2D plots represent a positive description of the real $I(\nu_1, \nu_2)$ values, at a 7% lowest contour. [Correction made here after initial online publication]

upon considering these data in magnitude mode are indicative of the presence of mixed-phase 2D line shapes. By contrast, when comparable single-scan 2D spectra are collected using the new amplitude-modulation scheme introduced in Fig. 1(B), line shapes that are free from dispersive components arise along the indirect domain and sharper, purely-absorptive features become available in the 2D traces along both domains (Fig. 2(B)). Similar gains are to be expected in other kinds of 2D NMR correlations.

Single-scan 2D NMR spectra from single-sweep encodings

A common feature of the encoding modes presented in Fig. 1 – and in fact of all encoding strategies heretofore proposed for carrying out single-scan 2D NMR – is their reliance on the use of $+G_e$ and $-G_e$ gradients of opposing amplitude. As mentioned this is needed for the sake of removing the quadratic z^2 term otherwise remaining in the spin evolution phases, which would prevent a *k*-driven refocusing of the type embodied by Eqn (3). These quadratic

terms were noted in Eqn (6) in connection to the execution of a single $\pi/2$ RF chirp; for the sake of clarity we rewrite this expression under the usual $O_i = -\gamma_e G_e L/2$, $R = \gamma_e G_e L/t^{(\pi/2)}$ conditions, as

$$\phi_{exc}(t^{(\pi/2)}, z) = (\Omega_1 + \gamma_e G_e z) \cdot t^{(\pi/2)} - \frac{(\Omega_1 + \gamma_e G_e z - O_i)^2}{2R}$$
$$= -\frac{\gamma_e G_e t^{(\pi/2)}}{2L} \cdot z^2 + \frac{(\gamma_e G_e L - 2\Omega_1)t^{(\pi/2)}}{2L} z$$
$$- \frac{(\gamma_e G_e L - 2\Omega_1)^2 t^{(\pi/2)}}{8\gamma_e G_e L} \tag{10}$$

Notice that the initial, z^2-dependent term is in fact independent of Ω_1, and thereby it is (i) spectroscopically uninformative, and (ii) the same for all sites in the sample. The question therefore arises of whether it would be possible to remove this term's undesired effects by a common post-acquisition manipulation, rather than by an active experimental refocusing. It turns that the answer to this is

Digitize and Rearrange

Phase correct along k

2D FT
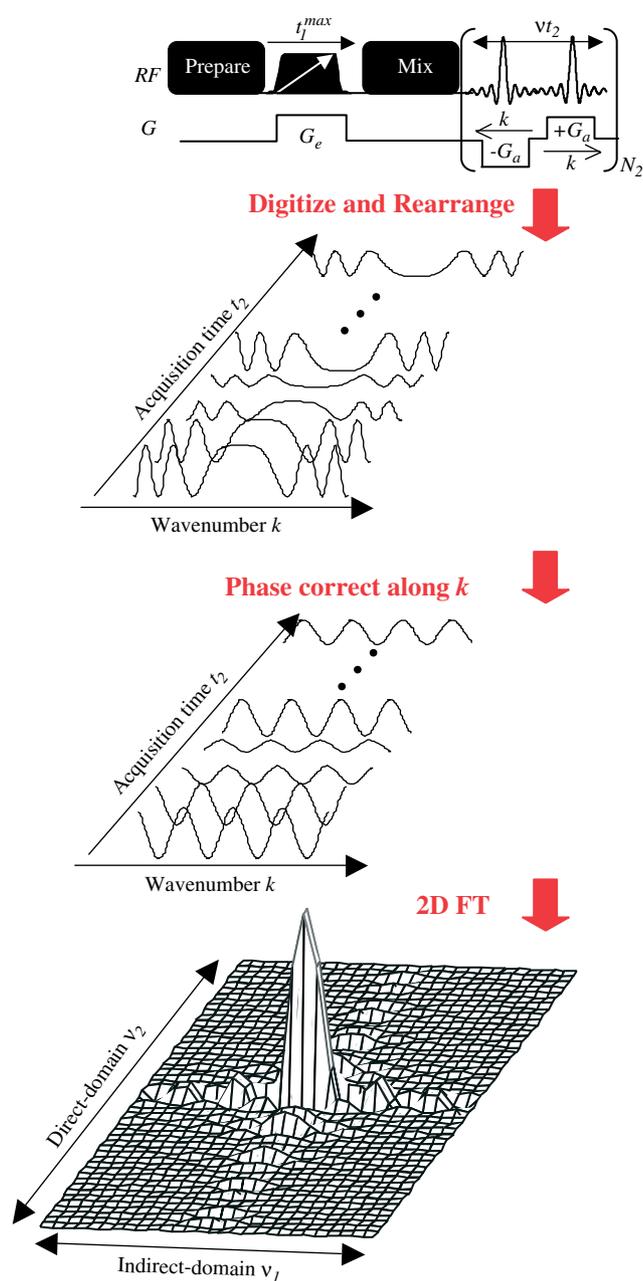
Figure 3. Top: new encoding scheme proposed for the execution of single-scan 2D NMR, based on the use of a single encoding-gradient/RF-pulse module. Bottom: various stages of data manipulation involved in the retrieval of the single-scan 2D spectrum including removal of the second-degree k dependence and 2D FT of the resulting $S(k, t_2)$ data, as described in the text.

involves a linear excitation sweep of the spins – even if other spatially incremented manipulations like storages or inversions could also be considered. The $\phi_{exc}(t^{(\pi/2)}, z)$ information encoded over t_1 will be preserved during a coherent mixing process, and then read-out by a train of oscillatory $\pm G_a$ gradients. Disregarding the effects of relaxation for the time being, the overall signal that will be detected from such sequence as a function of (k, t_2) can therefore be described as

$$S[k(t_2), t_2] \propto M(\Omega_1, \Omega_2) \int_{-L/2}^{+L/2}$$
$$\{\exp[i\phi_{exc}(z)] \exp[ik(t_2)z] \exp[i\Omega_2 t_2]\} dz \qquad (11)$$

where we consider for simplicity a single site characterized by $M(\Omega_1, \Omega_2)$, and have taken into account the fact that for a uniform sample this peak will not possess an explicit spatial dependence. Notice that by contrast to what happened with the sequences in Fig. 1 the approach shown in Fig. 3 leaves the quadratic z^2 term as part of the spins' t_1 spatial encoding ϕ_{exc}; no constructive echo will therefore arise among spin-packets at different z's, regardless of k-value. Instead, the resulting signal S will reflect at any given instant solely those spins located at a $z(k, t_2)$ coordinate that fulfills the stationary phase condition[22,24,25]

$$\frac{d}{dz}[\phi_{exc}(z) + k(t_2)z + \Omega_2 t_2]_{z=z(k,t_2)} = 0 \qquad (12)$$

for which spins positioned within a $\Delta z \approx \sqrt{\frac{R}{\gamma_e G_e}}$ distance, will lead to a locally-constructive interference among their magnetizations. On the basis of Eqn (10) it can be shown that the spins satisfying this condition will be centered at

$$z(k, t_2) = z_k = L\left(\frac{1}{2} + \frac{k}{\gamma_e G_e t^{(\pi/2)}}\right) - \frac{\Omega_1}{\gamma_e G_e} \qquad (13)$$

since the last term in this equation is small, this means that signals will arise in this experiment from the physically-meaningful $-L/2 \le z \le +L/2$ coordinates solely if k is swept between 0 and $k_{max} = -\gamma_e G_e t^{(\pi/2)}$ values. For simplicity we will assume that this range is indeed covered over the course of the acquisition, by pulsing a constant gradient G_a over a time T_a so that $\gamma_e G_e t^{(\pi/2)} + \gamma_a G_a T_a = 0$. Moreover, as $t^{(\pi/2)}$ and T_a will eventually become the t_1^{max} acquisition time and $\Delta t_2/2$ half t_2 dwell time of the 2D experiment, we shall also assume for the time being that the timing of this refocusing fulfills $T_a \ll t^{(\pi/2)}$. With all these assumptions, Eqn (11) predicts an observable signal

$$S(k, t_2) \propto \Delta z \cdot M(\Omega_1, \Omega_2) \cdot \exp\{i[\phi_{exc}(z_k) + k \cdot z_k]\}$$
$$\cdot \exp[i\Omega_2 t_2] \qquad (14)$$

Inserting now the explicit form taken by z_k (Eqn (13)) into both this equation and in the ϕ_{exc} function of Eqn (6) yields the explicit (k, t_2)-dependence of this signal:

$$S(k, t_2) \propto \Delta z \cdot M(\Omega_1, \Omega_2) \cdot \exp\left[i\frac{L}{2\gamma_e G_e t^{(\pi/2)}}k^2\right]$$
$$\exp\left[i\frac{L}{2}k\right] \cdot \exp\left[i\frac{\Omega_1}{\gamma_e G_e}k\right] \cdot \exp[i\Omega_2 t_2] \qquad (15)$$

The first exponential in this expression, involving a quadratic phase term varying as k^2, is not usually present in ultrafast

actually positive, provided that signals are observed during t_2 while subjecting the spins to an acquisition-gradient $G_a \ne G_e$. In that case the relative contributions of the initial encoding gradient G_e and of Ω_1 to the overall indirect-domain frequencies – appearing in Eqn (10) as a single $(\gamma_e G_e L - 2\Omega_1)$ term – can be told apart, and 2D NMR spectra be obtained using a single $\pi/2$ swept pulse as the sole t_1 spatial encoding event. The present paragraph briefly focuses on exploring this new alternative.

The overall scheme of the protocol to be considered is summarized in Fig. 3. It consists of a 2D sequence where t_1

Magnetic
Resonance in
Chemistry

Mixing-less correlation

TOCSY-based correlation

Figure 4. 2D homonuclear correlations observed in a single scan on an *n*-butylchloride/CDCl$_3$ solution utilizing the indicated mixing-less (left) and TOCSY-based (right) pulse sequences. Gradients are in G/cm and durations in ms; additional experimental parameters included a 4.75-kHz sweep in the $\pi/2$ excitations, physical acquisition dwell times of 6.25 μs, 5-μs gradient recovery times, 3200 overall acquisition points and a 10-kHz DIPSI bandwidth. The processing of the resulting 1D FIDs followed the summary in Fig. 3: data rearrangement in the (k, t_2)-space, quadratic phase correction along k, 2D FT, and magnitude-mode data calculation.

(A) Single-scan 2D HSQC - Urea

(B) Single-scan 2D HSQC - LeuAlaPhe
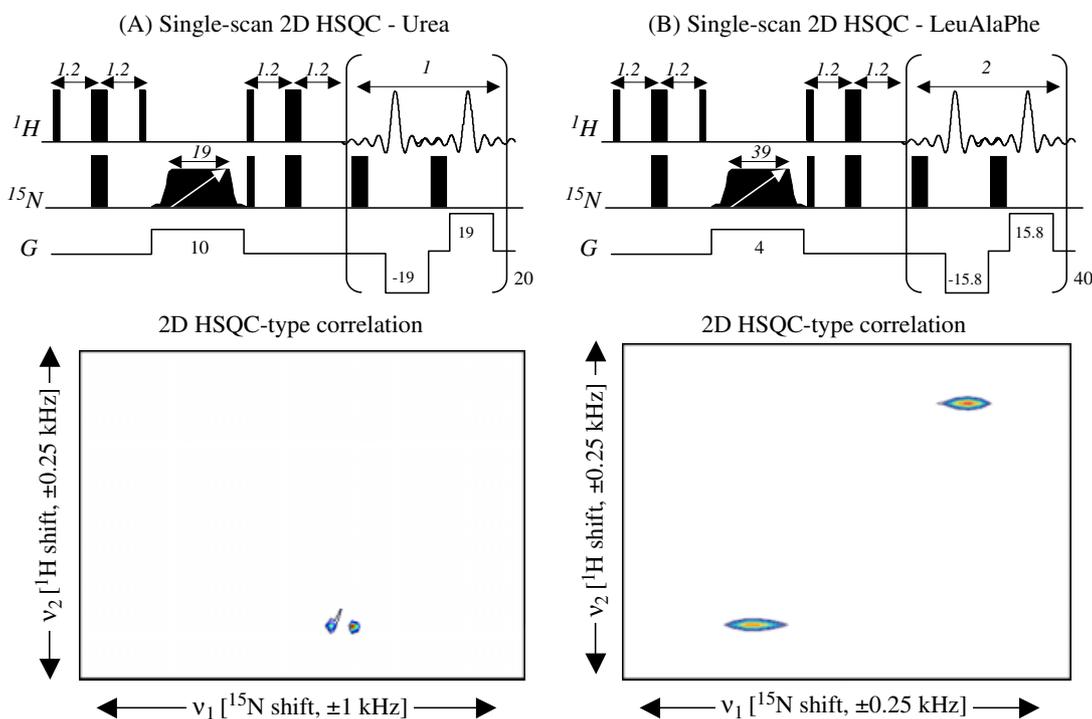
Figure 5. Idem as Fig. 4, but for a single-scan 2D HSQC experiment performed on: (A) a 40-mM ^{15}N-labeled urea sample, and (B) a 2-mM solution of the ^{15}N-labeled LeuAlaPhe tripeptide; both of these dissolved in d_6-DMSO. Narrow and broad bars indicate non-selective $\pi/2$ and π pulses respectively; the encoding $\pi/2$ pulse was chirped over 8 kHz to excite the ^{15}N anti-phase evolution, and a train of ^{15}N π pulses included in the acquisition for decoupling purposes.

2D experiments. It is, however, common for all sites in the sample and only depends on experimental values under *a priori* control; it can therefore be removed from the collected signal by post-processing. So can the $\exp[i(L/2)k]$ phase modulation involved in the second exponential term, also common to all sites. The remaining terms in the phasor include the Ω_1- and

Ω_2-dependencies that one is attempting to obtain; Eqn (15) suggests that for a general multi-site case their governing spectral distribution can be retrieved by doing a 2D FT of the signal against the (k, t_2) variables. In other words, this model suggests that Fig. 3 can yield a general 2D NMR spectrum $l(\nu_1, \nu_2)$ if data are acquired upon subjecting the spins to a $\pm G_a$-driven
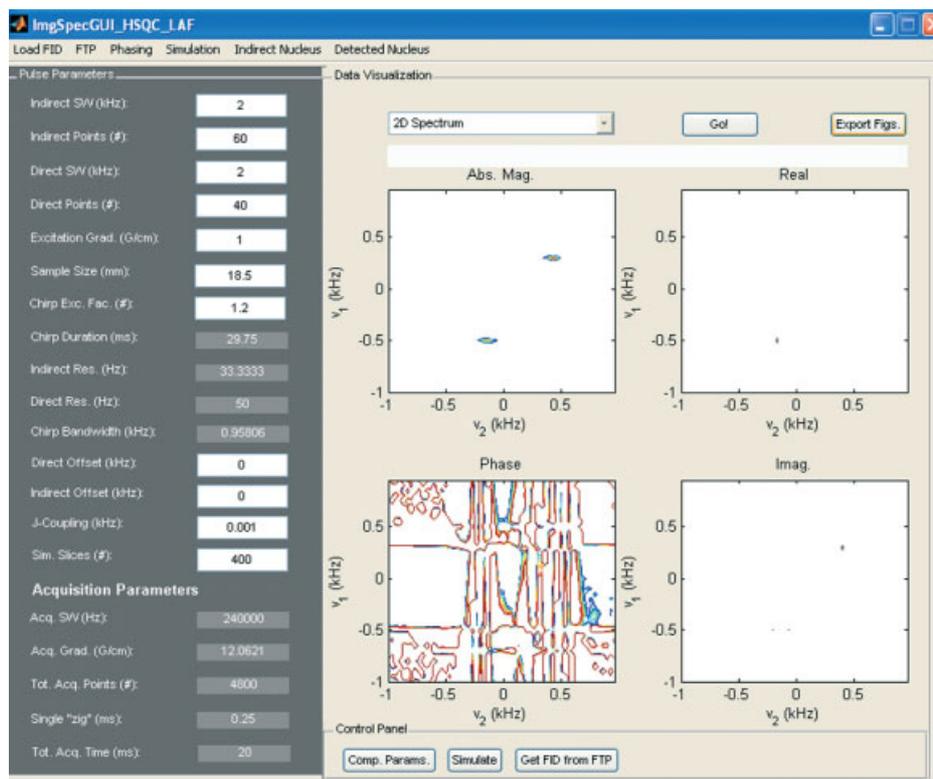
Figure 6. Example of the kind of control script written for setting up the acquisition, post-processing and simulation of single-sweep single-scan 2D NMR data (available upon request).

oscillation in conjunction with a monotonic incrementation of the t_2 – i.e. by implementing a standard Echo-Planar Spectroscopic Imaging acquisition.[26] This signal then needs to be freed from the unwanted (and uninformative) k- and k^2-terms just highlighted, and finally subject to a 2D FT processing in the resulting (k, t_2) plane.

It is enlightening to expand some of the technical aspects of this new single-sweep approach to retrieve ultrafast 2D NMR data, primarily how the various parameters involved in the experiment will help define the spectral characteristics. Given the traditional $\exp[i\Omega_2 t_2]$ modulation appearing in Eqn (15), the direct-domain spectral properties will be as in traditional Fourier NMR: spectral widths will be characterized by $1/(2T_a)$ – or $1/T_a$ if an interlaced fast FT is used[27,28] – and resolution will be proportional to the inverse of the overall acquisition time $2N_2 T_a$ used in the sampling. The indirect-domain information, by contrast, is supported by the much shorter times T_a over which the quadratic-phase 'imaging' information encoded by the initial $\pi/2$ chirp pulse is actually read out. To appreciate the compatibility between this read-out interval and the usual demands of high-resolution spectroscopy one can rewrite the Ω_1-dependent modulation of Eqn (15) as $\exp\left[-i\left(\Omega_1 \frac{\gamma_a G_a}{\gamma_e G_e}\right)t\right]$, where now $0 \leq t \leq T_a$ defines the progress of the k-variable to be FT'd. The $\gamma_e G_e t^{(\pi/2)} + \gamma_a G_a T_a = 0$ condition allows one to further simplify this expression into $\exp[i\Omega_1 t']$, where $0 \leq t' \leq t^{(\pi/2)}$. It follows that the spectral resolution along the indirect domain will be given, as in conventional 2D NMR spectroscopy,[2] by the inverse of the overall encoding time $t^{(\pi/2)}$; whereas the width SW_1 of indirect-domain spectral frequencies that can be suitably characterized will be defined by the number of N_1 points sampled within each T_a interval: $SW_1 = \frac{N_1}{t^{(\pi/2)}}$. [For completion one should add that if the $T_a \ll t^{(\pi/2)}$ condition is

broken and one can no longer assume that the evolution effects introduced by Ω_2 over the course of each T_a were negligible, the indirect-domain frequencies afforded by this FT procedure become $\Omega_{ind} = \Omega_1 - \Omega_2 \frac{T_a}{t^{(\pi/2)}}$. Still, since the direct-domain provides an independent measure of the Ω_2's, 'pure' $I(\nu_1, \nu_2)$ distributions can be retrieved by shearing the 2D spectral data.]

The single-sweep encoding strategy just outlined was tested with a couple of complementary experiments. In one of these the same n-butylchloride sample as analyzed in the previous Paragraph was subjected to the single-sweep encoding protocol, toward the acquisition of homonuclear 2D spectra within a single scan. The pulse sequences and parameters used, together with the resulting $I(\nu_1, \nu_2)$ spectra, are summarized in Fig. 4. Though not possessing the highest of resolution (partly due to their magnitude-mode mixed-phase format), the expected diagonal- and cross-peak features are easily recognizable. One point worth noticing in these experiment is the weak gradient strength chosen for the encoding process; this is a consequence of the high G_a strengths otherwise dictated by the $\gamma_e G_e t^{(\pi/2)} + \gamma_a G_a T_a = 0$ condition, as well as by unnecessary sensitivity losses otherwise expected by diffusion over the course of the encoding.[29,30] Fig. 5 illustrates another set of this new single-sweep encoding protocol applications, this time to the collection of a single-transient 2D ^{15}N–^1H correlations based on the HSQC indirect-detection method.[31] Notice once again the simplicity of the sequence. Since no ^1H decoupling was applied during t_1 a heteronuclear J_{NH}-coupling pattern is observed along the indirect domain of Fig. 5(A); this pattern was masked in Fig. 5(B) by apodization of the data. For completion Fig. 6 presents an outline of the interphase

controlling the Matlab® script that was written in order to process this kind of spectra.

Conclusions

The present study discussed two new encoding modes aimed at increasing the flexibility of single-scan 2D NMR. The first one modified a traditional double-sweep amplitude-modulated approach, so as to improve both the phasing and the dispersive-component characteristics of its spectral line shapes. The resulting performance was good and, although sensitivity-wise the results may not have been as impressive as the gains available from other encoding modes (like the double-frequency sweep in Ref. [18]), it was found that setting up this new encoding mode was substantially easier than setting the latter sequence. The second proposal in work, based on implementing the spatial encoding underlying single-scan 2D NMR by performing a single-pulse RF sweep, presented a more radical departure of traditional encoding modes, and therefore opens a number of intriguing options whose potential remains to be explored. It is clear that from an experimental standpoint this approach simplifies even further the realization of ultrafast 2D experiments, as it replaces the need for having $\pm G_e$ gradient oscillations by a single manipulation followed by a data-processing stage that accounts numerically for unwanted evolution terms. Moreover, it appears that this single-sweep approach can be implemented in a number of manners that differ from the one treated in Figs 3–5, including single π-pulse swept inversions, symmetric chirped excitations or constant acquisition-gradient modes simplifying even further the experimental protocol. At the same time, it remains to be seen to what extent is the sensitivity of these new encoding options affected by relaxation and motional losses, *vis-à-vis* hitherto proposed alternatives. We trust to clarify these various features further in upcoming studies.

References

[1] J. Cavanagh, W. J. Fairbrother, A. G. Palmer III, N. J. Skelton, M. Rance, Protein NMR Spectroscopy: Principles and Practice, **2006**.

[2] R. R. Ernst, G. Bodenhausen, A. Wokaun, Principles of Nuclear Magnetic Resonance in One and Two Dimensions, **1990**.

[3] K. Schmidt-Rohr, H. W. Spiess, Multidimensional Solid-State NMR and Polymers, **1994**.

[4] J. Jeener, Ampere international summer school ii, in *Basko Polje, Yugoslavia. Lecture Notes Published in "NMR and More in Honor of Anatole Abragam"* (Eds: M. Goldman, M. Porneuf), (Les editions de physique, Les Ulis, France, 1994), **1971**.

[5] W. P. Aue, E. Bartholdi, R. R. Ernst, *J. Chem. Phys.* **1976**, *64*, 2229.

[6] E. Kupče, T. Nishida, R. Freeman, *Prog. Nucl. Magn. Reson. Spectrosc.* **2003**, *42*, 95.

[7] H. S. Atreya, T. Szyperski, *Methods Enzymol.* **2005**, *394*, 78.

[8] J. C. Hoch, A. S. Stern, *Methods Enzymol.* **2001**, *338*, 159.

[9] L. Frydman, T. Scherf, A. Lupulescu, *Proc. Natl. Acad. Sci. U.S.A* **2002**, *99*, 15858.

[10] L. Frydman, A. Lupulescu, T. Scherf, *J. Am. Chem. Soc.* **2003**, *125*, 9204.

[11] L. Frydman, *Comptes Rendus Chimie* **2006**, *9*, 336.

[12] Y. Shrot, B. Shapira, L. Frydman, *J. Magn. Reson.* **2004**, *171*, 163.

[13] Y. Shrot, L. Frydman, *J. Chem. Phys.* **2008**, *128*, 052209.

[14] B. Shapira, A. Lupulescu, Y. Shrot, L. Frydman, *J. Magn. Reson.* **2004**, *166*, 152.

[15] P. Pelupessy, *J. Am. Chem. Soc.* **2003**, *125*, 12345.

[16] N. S. Andersen, W. Köckenberger, *Magn. Reson. Chem.* **2005**, *43*, 795.

[17] A. Tal, B. Shapira, L. Frydman, *J. Magn. Reson.* **2005**, *176*, 107.

[18] B. Shapira, Y. Shrot, L. Frydman, *J. Magn. Reson.* **2006**, *178*, 33.

[19] P. Giraudeau, S. Akoka, *J. Magn. Reson.* **2007**, *186*, 352.

[20] M. Gal, L. Frydman, *Encyclopedia Magn. Reson.* **2009**, *10*, in press.

[21] J. M. Böhlen, M. Rey, G. Bodenhausen, *J. Magn. Reson.* **1989**, *84*, 191.

[22] Y. Shrot, L. Frydman, *J. Magn. Reson.* **2005**, *172*, 179.

[23] J. Cavanagh, M. Rance, *J. Magn. Reson.* **1992**, *96*, 670.

[24] A. Tal, L. Frydman, *J. Magn. Reson.* **2006**, *182*, 179.

[25] A. Tal, L. Frydman, *J. Magn. Reson.* **2007**, *189*, 46.

[26] P. Mansfield, *Magn. Reson. Med.* **1984**, *1*, 370.

[27] G. Metzger, X. Hu, *J. Magn. Reson.* **1997**, *125*, 166.

[28] M. Mishkovsky, L. Frydman, *J. Magn. Reson.* **2005**, *173*, 344.

[29] P. Giraudeau, S. Akoka, *J. Magn. Reson.* **2008**, *192*, 151.

[30] Y. Shrot, L. Frydman, *J. Chem. Phys.* **2008**, *128*, 164513.

[31] G. Bodenhausen, D. J. Ruben, *Chem. Phys. Lett.* **1980**, *69*, 185.

422